THE ASTROPHYSICAL JOURNAL, 290:671–682, 1985 March 15

HIGH-VELOCITY WINDS IN CLOSE BINARIES WITH ACCRETION DISKS. II. THE VIEW ALONG THE PLANE OF THE DISK

FRANCE A. CÓRDOVA
University of California, Los Alamos National Laboratory

AND

KEITH O. MASON
University College London, Mullard Space Science Laboratory
Received 1984 May 29; accepted 1984 October 4

ABSTRACT

We present phase-resolved, ultraviolet spectra of the eclipsing cataclysmic binaries RW Trianguli and DQ Herculis. Both stars display N v λ1240, Si iv λ1400, C iv λ1549, and He ii λ1640 in emission. The strongest spectral feature in both stars is C iv λ1549. In RW Tri this line has an equivalent width of 40 Å (out of eclipse), a FWHM of 13 Å, and is asymmetric with the peak displaced redward of the line centroid by 4 Å; the blue wing of the line extends to velocities of -3000 km s^{-1}. The C iv line in DQ Her has an equivalent width of 110 Å (out of eclipse), and a FWHM of 9.5 Å; the out-of-eclipse line profile is not obviously asymmetric, but the eclipse profile is skewed redward of line center. In both stars there is a deep eclipse of the UV continuum, representing an occultation of the interior regions of an accretion disk surrounding the degenerate dwarf. None of the spectral lines in either binary system are eclipsed to the same degree as the UV continuum, indicating that the lines are formed in an extended region above and below the disk. The distinctive morphology of RW Tri's lines suggests an origin in an accelerating wind. The observed hard X-ray flux from RW Tri is not sufficient to drive the wind, but UV and/or EUV radiation from the inner disk could provide the required energy. The continuum spectrum of RW Tri is significantly reddened, with $E(B-V) = 0.25$; this result when combined with previous measurements of the surface brightness distribution of RW Tri's disk yields a mass accretion rate of about 10^{18} g s^{-1}.

Subject headings: stars: accretion — stars: eclipsing binaries — stars: individual — ultraviolet: spectra

I. INTRODUCTION

An unanticipated result of ultraviolet observations of close binary systems with luminous accretion disks was the detection of high-velocity winds (Hutchings 1980; Krautter *et al.* 1981; Córdova and Mason 1982; Guinan and Sion 1982; Greenstein and Oke 1982; Szkody 1982; Klare *et al.* 1983). The correlation of a wind with times of high disk luminosity suggests that radiative pressure in the lines may play a role in accelerating the wind (Córdova and Mason 1982, hereafter Paper I). The high-energy X-ray and EUV emission resulting from the gravitational accretion energy liberated in the inner disk provides a ready source of ionizing photons. In this paper we investigate the location and geometry of the wind by examining the phase-related behavior of the UV line profiles in two cataclysmic variable stars, RW Trianguli and DQ Herculis, which are viewed along the plane of the disk.

RW Tri is a novalike variable with a 5.57 hour binary period and a high inclination (Kaitchuck, Honeycutt, and Schlegel 1983 find $i = 85°$; see also Frank and King 1981). DQ Herculis is an ex-nova with a binary period of 4.65 hours and is viewed at an inclination close to 90° (Petterson 1980; Young and Schneider 1980). Using the *International Ultraviolet Explorer Satellite* (*IUE*), we obtained complete orbital phase coverage, including five eclipses, of RW Tri, and partial phase coverage, including one eclipse, of DQ Her. These observations complement the UV phase-resolved spectrophotometry of another short-period, eclipsing, novalike variable, UX Ursae Majoris (Holm, Panek, and Schiffer 1981; King *et al.* 1983).

Section II of this paper describes our ultraviolet observations and analysis techniques and the collection of simultaneous optical data on both stars. In § III representative UV spectra of the two systems are shown, and their continuum energy distributions are discussed in terms of accretion disk models. In § IV the optical and UV continuum light curves are presented as a function of energy. The line profiles in and out of eclipse are compared in § V. The observations are interpreted as evidence for a high-velocity wind in § VI, where the relationship of the line emission to the observed X-ray spectrum is also discussed. The conclusions are summarized in § VII.

II. THE OBSERVATIONS AND ANALYSIS

a) Ultraviolet

Table 1 summarizes the observations of RW Tri and DQ Her which were made using the low-resolution spectrographs on *IUE*. The table includes the orbital phase intervals covered during each exposure. The phase convention used for RW Tri is discussed below. For DQ Her the phases are based on the ephemeris of Pringle (1975). For both stars phase 0.0 corresponds to the minimum in the optical light curve. The heliocentric ephemerides have been converted to Universal Time.

We observed RW Tri with *IUE* on 1982 January 13, 14, and 18 and on 1982 August 7. In all, 29 spectra with exposure times ranging between 10 and 36 minutes were taken. The January 13/14 observations cover the orbital phase interval 0.9 to 1.4 on two successive cycles, while the January 18 observations cover phases 0.4 to 1.1. The August 7 spectra were taken during two eclipses and span the phase interval 0.9 to 1.3.

Six spectra of DQ Her were taken with 40–60 minute time resolution; three on 1982 August 5 and three on 1982 August 7,

TABLE 1

LOG OF *IUE* OBSERVATIONS

Sequence Number	Camera	Date (1982)	Start (UT)[a]	Duration (minutes)	Orbital Phase Interval	Phase Center	Comments on Image Quality
			RW Trianguli				
16037a	SWP	Jan 13	23^{h}05^m 40^s	29.3	0.86–0.95	0.91	
16037b	SWP	Jan 13	23 35 (00)	25	0.95–1.02	0.99	
12335	LWR	Jan 14	0 09 48	25	1.05–1.13	1.09	
16038a	SWP	Jan 14	0 40 34	25	1.14–1.22	1.18	bad from λλ1470–1485
16038b	SWP	Jan 14	1 05 35	25	1.22–1.30	1.26	high background, very noisy
12336	LWR	Jan 14	1 39 43	35	1.32–1.43	1.38	
12337	LWR	Jan 14	4 51 18	10	1.90–1.93	1.91	
16040a	SWP	Jan 14	5 08 47	25	1.95–2.02	1.99	
16040b	SWP	Jan 14	5 34 (00)	25	2.02–2.10	2.06	
12338	LWR	Jan 14	6 06 45	25	2.12–2.20	2.16	
16041a	SWP	Jan 14	6 37 35	25	2.21–2.29	2.25	bad for $\lambda < 1270$
16041b	SWP	Jan 14	7 02 (00)	25	2.29–2.36	2.32	bad for $\lambda < 1310$; ion hit λ1400
12339	LWR	Jan 14	7 33 48	15	2.38–2.43	2.41	
16063	SWP	Jan 18	0 38 24	32	0.39–0.49	0.44	bad for $\lambda < 1310$
12356	LWR	Jan 18	1 14 20	25	0.50–0.57	0.54	
16064a	SWP	Jan 18	1 43 29	36	0.58–0.69	0.64	
16064b	SWP	Jan 18	2 19 (30)	36	0.69–0.80	0.75	
12357a	LWR	Jan 18	3 00 14	20	0.81–0.87	0.84	
12357b	LWR	Jan 18	3 20 (00)	20	0.87–0.93	0.90	
16065a	SWP	Jan 18	3 46 12	25	0.95–1.02	0.99	
16065b	SWP	Jan 18	4 11 11	25	1.02–1.10	1.06	
17617a	SWP	Aug 7	10 08 (00)	10	0.90–0.93	0.92	
17617b	SWP	Aug 7	10 18 (00)	10	0.93–0.96	0.95	
17617c	SWP	Aug 7	10 28 (00)	10	0.96–0.99	0.98	
13887	LWR	Aug 7	15 24 36	30	1.85–1.94	1.89	
17620a	SWP	Aug 7	16 01 57	10	1.96–1.99	1.98	
17620b	SWP	Aug 7	16 11 54	10	1.99–2.02	2.01	
13888	LWR	Aug 7	16 44 23	25	2.09–2.16	2.13	
17621	SWP	Aug 7	17 14 20	35	2.18–2.28	2.23	
			DQ Herculis				
13864	LWR	Aug 5	05 51 15	60	0.52–073	0.62	
17593a	SWP	Aug 5	07 00 21	40	0.76–0.91	0.83	partially occulted by slit
17593b	SWP	Aug 5	07 48 03	40	0.93–1.08	1.00	
17614a	SWP	Aug 7	02 36 22	60	0.15–0.36	0.25	partially occulted by slit
17614b	SWP	Aug 7	03 35 58	60	0.36–0.57	0.47	
17615	SWP	Aug 7	05 41 07	40	0.81–0.95	0.88	

[a] Times in parentheses uncertain to ~10 s.

over portions of two orbital cycles, including one spectrum centered exactly on the optical eclipse.

All the UV spectra were taken with an aperture of 10″ × 20″ and had a resolution of ~6 Å in the short-wavelength camera (SWP: 1150–1950 Å) and ~9 Å in the long-wavelength camera (LWR: 1950–3100 Å). Many of the images contain multiple spectra; these are noted in Table 1 (e.g., SWP 16037 contains the two exposures 16037a and 16037b). These spectra were displaced in position from each other along the direction perpendicular to the dispersion. Given the size of the aperture in this direction (20″) and the point source resolution of the low-dispersion cameras (~4″), spectra positioned ~11″.8 apart are easily resolvable and can be analyzed using the data file on the Goddard Space Flight Center Guest Observer tape that contains 55 extracted lines ("orders") comprising the image on the camera. To reduce the double spectra we summed the five brightest orders for each spectrum of RW Tri and four orders for the fainter DQ Her spectra. The orders summed for the two spectra did not overlap. By comparing five line summations with nine line summations (i.e., as used in the standard GSFC analysis) of single spectra, we estimate that about 4% of the light is lost in the former. To facilitate intercomparison, we also summed five orders for the single spectra we obtained so that the fraction of the total light registered in each spectrum was about the same. In one instance (SWP 17617) we exposed three spectra on the same image. These spectra were so close (~5″.6) that they could not be resolved; these data were discarded.

Table 1 includes comments about the image quality. RW Tri was positioned in the slit using the *IUE* Fine Error Sensor (FES) (see below); comparison of the spectra with the image of the geocoronal Lyα (i.e., using the "photowrites") showed that the spectra were well centered in the slit in the direction perpendicular to the dispersion. DQ Her, on the other hand, was too faint to be acquired with the FES and was positioned by offsetting the spacecraft from a nearby SAO star. The doubly exposed images of DQ Her were not well positioned, causing the first image of each double exposure to fall partially beyond the edge of the slit. These spectra were not used in the analysis described below.

b) Optical

i) *RW Trianguli*

The FES on *IUE* can be used as an optical photometer to estimate a star's visual magnitude, given its $B-V$ color. For

RW Tri we recorded the FES count rate before and after every UV exposure. The accuracy of this photometry is ± 0.1 mag (Holm and Crabb 1979). The light curve assembled from these data shows the source to be constant in the V band to within about 10%. We derive a mean flux at 5400 Å of $\sim 2 \times 10^{-14}$ ergs cm^{-2} s^{-1} Å^{-1} ($V = 13.2$, assuming $B-V = 0.25$).

Ground-based optical photometry of RW Tri was obtained by Dr. John Middleditch on 1982 January 15 (i.e., between the 1982 January 14 and January 18 *IUE* observations). An EMI 9658A phototube was used on the 1.5 m NASA/University of Arizona telescope on Mount Lemmon, Arizona. The optical observations cover a portion of one orbital cycle ($\phi = 0.82$–1.14), including the eclipse at $\phi = 0.0$. Their purpose was to update the epoch of eclipse, measure the eclipse depth as a function of color, and acquire time-averaged *UBVRI* magnitudes to extend the spectral coverage of the ultraviolet measurements. Standard Johnson *UBVRI* filters were used with a 26″ aperture in 2″–4″ seeing. The data were recorded continuously with 1 s integrations. An automatic system moved the telescope between star and sky every ~ 20 s. At intervals of several minutes the filter wheel was manually rotated to give sequential *UBVRI* measurements.

The epoch of mid-eclipse derived from the single observed optical eclipse is HJD 2,444,984.6562. This coincides exactly with Mandel's (1965) ephemeris. Such a close coincidence might be fortuitous, since Africano *et al.* (1978) have shown that the eclipse timings of RW Tri are not consistent with a constant or linear ephemeris. Our ephemeris is not in error by more than ~ 0.01 in phase at the epoch of the UV observations, sufficiently accurate given the time resolution of the UV data.

We reduced the Mount Lemmon photometry by comparing the sky-background-subtracted measurements of RW Tri with similar measurements of two of Landolt's standard stars, 96−615 and 102−616 (Moffett and Barnes 1979) and using the mean atmospheric extinction values appropriate for Mount Lemmon at the time of the observations. The out-of-eclipse colors for RW Tri are $V = 13.12 \pm 0.02$, $B-V = 0.25 \pm 0.04$, $U-B = 0.67 \pm 0.03$, $V-R = 0.44 \pm 0.02$, and $R-I = 0.27 \pm 0.07$. The errors are the standard errors only. The nonsimultaneity of the color measurements coupled with the ubiquitous flickering of this star contributes an additional source of uncertainty. The measurement of V is within 0.1 mag of the mean FES measurements made on proximate days.

The data provide the following approximate magnitudes for the eclipse depths: 1.98 mag in U; 1.95 mag in B; 1.65 mag in V; 1.35 mag in R; and 1.05 mag in I.

ii) *DQ Herculis*

Spectra of DQ Her were taken near the time of the *IUE* observations by Dr. J. Clarke using the Image Dissector Scanner on the Anna Nickel 1 m telescope at Lick Observatory. The spectra were obtained with an 8″ aperture in 2″ seeing, covered the wavelength interval 3500–7500 Å, and had a spectral resolution of about 10 Å. Spectra were obtained 1982 August 5 between 06:03 and 07:21 U.T. (binary phase $\phi \approx 0.69$), and 1982 August 9 between 04:49 and 05:24 U.T. ($\phi \approx 0.01$), and 05:59 and 06:17 U.T. ($\phi \approx 0.23$). Clarke's reduced B, V, and R magnitudes for DQ Her on August 5 are 14.82, 14.53, and 14.27, respectively. On August 9, $V = 15.34$ outside of eclipse. He II was somewhat stronger than Hβ in all spectra: The strength of He II on August 5 was $\sim 1.7 \times 10^{-13}$ ergs cm^{-2} s^{-1}, while the strength of Hβ was $\sim 1.1 \times 10^{-13}$ ergs cm^{-2} s^{-1}. The August 9 spectral line fluxes in and out of eclipse are discussed in § V*b*.

III. SPECTRUM

a) UV Spectral Features

i) *RW Trianguli*

Selected individual SWP spectra of RW Tri taken on 1982 January 18 are shown in Figure 1. They represent complete orbital phase coverage, including the eclipse. The 1982 January 14 spectra, which are not shown, do not differ qualitatively from these. All of the RW Tri spectra taken on 1982 August 7 are illustrated in Figure 2; the top two panels, which cover the eclipse ingress and midpoint, were taken with exposure times of only 10 minutes and no time gap between them, representing the highest time resolution UV data obtained on this star. Figure 2 has been smoothed with a five-point triangular-shaped filter, but no smoothing has been applied in Figure 1.

Several spectra lines are seen in emission: their wavelengths and probable identifications are λ1176 (C III), λ1240 (N V), λ1400 (Si IV), λ1549 (C IV), and possibly λ1640 (He II). There are absorption features at λ1302 (O I and/or Si II, or Si III), and possibly also at λ1260 (S II and/or Si II). In some spectra weak features are seen between λ1465 and λ1495 which could be emission, or absorption, or both, and may be weak lines of S I and/or Ni II. A feature at λ1280 could be Si III or C I in emis-

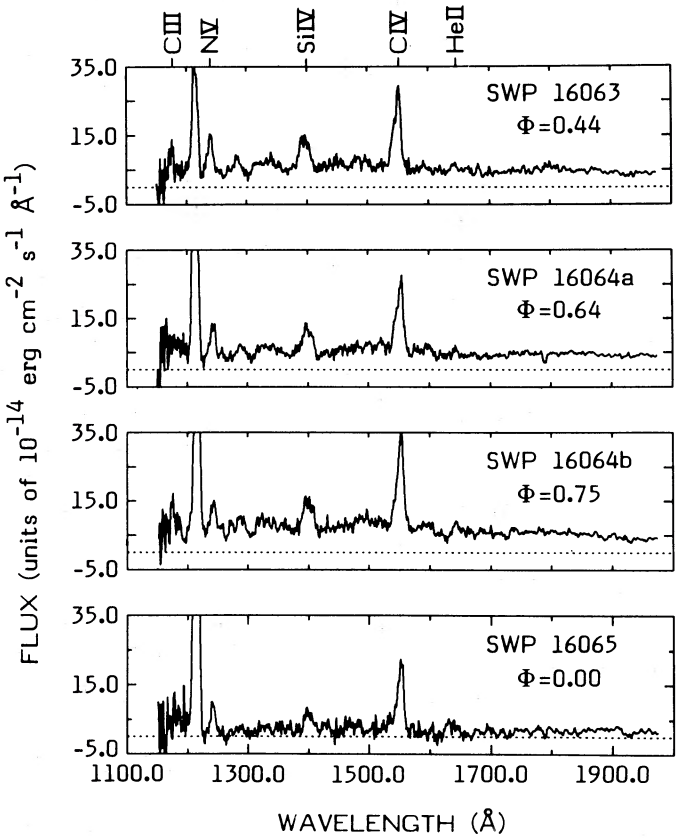

FIG. 1.—Representative *IUE* spectra of RW Trianguli taken at various binary orbital phases on 1982 January 18. Zero background level is denoted with a short dashed line in this and subsequent figures. The emission lines are prominent even during the eclipse of the continuum ($\phi = 0.0$). See Table 1 for details about exposure times, etc.

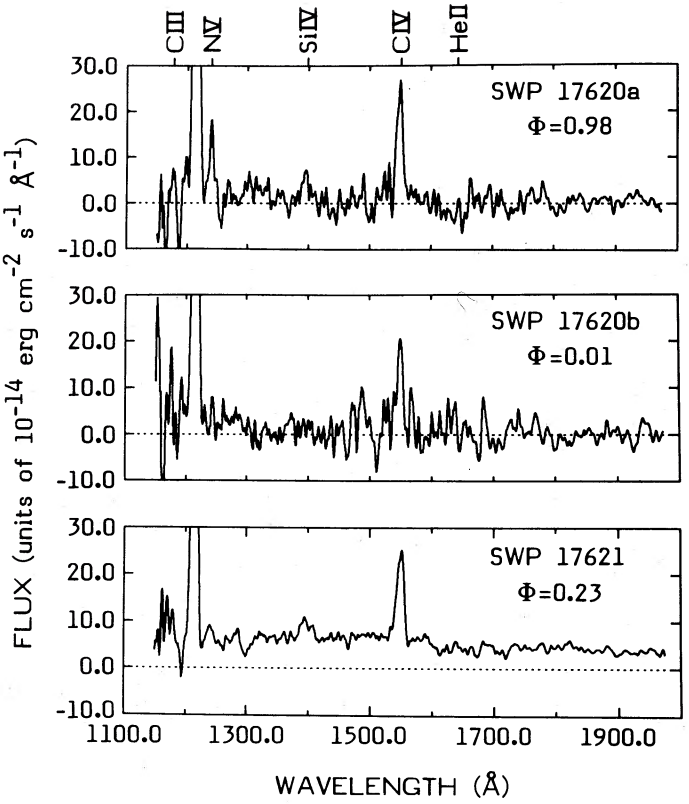

FIG. 2.—*IUE* spectra of RW Trianguli taken on 1982 August 7 with a higher time resolution than represented in Fig. 1. See Table 1 for details.

sion, or the result of the absorption features at λ1260 and λ1300.

The continuum spectra of SWP 16063, 16064a, and 16064b show a wavy pattern with troughs 50–100 Å wide, centered at Lyα, Si IV, and $\sim\lambda$1670 (see Figs. 1*a*, 1*b*, and 1*c*). These "absorption valleys" are reminiscent of the model atmospheres for hot, high-gravity stars (Wesemael *et al.* 1980). They are prominent only in spectra taken at orbital phases between 0.4 and 0.8, but since these phases were sampled only once we cannot claim a correlation with orbital phase.

The long wavelength spectra are nearly featurless except for a broad dip centered at about 2200 Å (described in § III*b*) and a emission-like feature at λ1985; these spectra are not displayed here. Mg II λ2802, a common feature in similar systems, is not observed in the superposition of all LWR spectra but may be weakly present in three individual spectra (LWR 12336, 12338, and 12339) of 1982 January 14.

In Table 2 we list the average fluxes (or upper limits) and equivalent widths of the lines, discriminating between eclipse and out-of-eclipse spectra.

ii) *DQ Herculis*

All three good-quality SWP spectra of DQ Her are shown in Figure 3, including the spectrum taken during an eclipse; the data have been smoothed with a five-point triangular-shaped filter. N V, Si IV, C IV, and He II are in emission. The fluxes and equivalent widths are listed in Table 2. The single LWR spectrum of DQ Her (not shown) is quite faint, and no spectral lines are detectable.

TABLE 2

UV EMISSION-LINE FLUXES[a] AND EQUIVALENT WIDTHS

Eclipse		N V	Si V	C IV	He II	Mg II	
RW Trianguli							
Yes	flux	7.5	8	21	≤1.4	...	
	EW (Å)	100	50	120	≤11	...	
No	flux	9.4	18	27	1.4	≤1.7	
	EW (Å)	21	32	40	3	≤5	
DQ Herculis							
Yes	flux	1.9	1.1	6.7	≤0.8	...	
	EW (Å)	~145	~100	~280	≤25	...	
No	flux	4.8	3.4	13.5	2.7	≤0.7	
	EW (Å)	60	30	110	30	≤8	

[a] Units of 10^{-13} ergs cm^{-2} s^{-1}, not corrected for reddening.

b) Energy Distribution from 1200 Å to 22000 Å

i) *RW Trianguli*

To calculate the integrated flux of the star and fit spectral models to the energy distribution we summed the 1982 January out-of-eclipse spectra (orbital phase 0.15–0.85) in bins of 50 Å to 100 Å width, avoiding spectral lines, spurious features (as determined from the photowrites), and SWP 16038b which was noisy due to high radiation background. The revised *IUE* calibration of Finley, Basri, and Bowyer (1984) has been adopted. (We note that the chief effects of this revised calibration are to flatten the spectrum and decrease $E(B-V)$

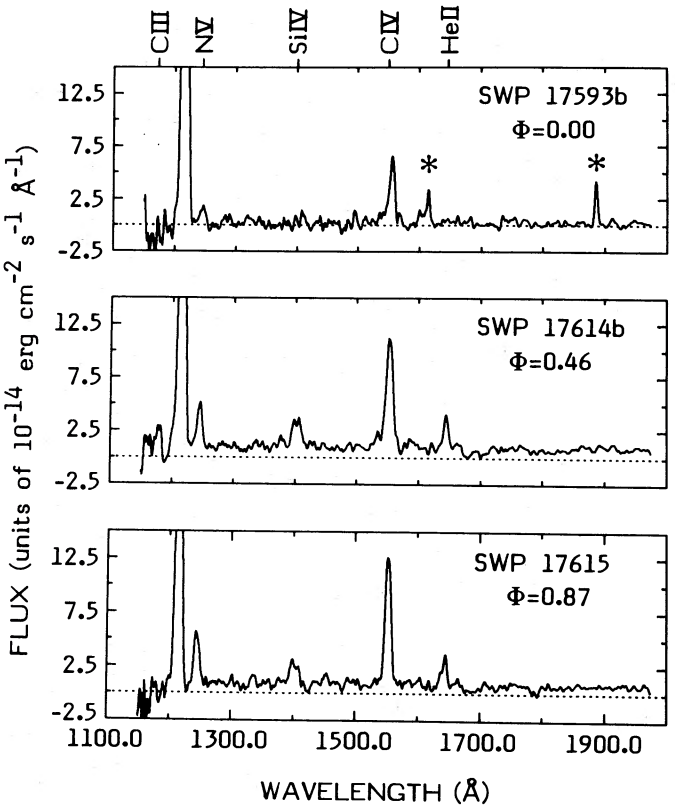

FIG. 3.—*IUE* spectra of DQ Herculis taken on 1982 August 5 and August 7. As with RW Tri, the emission lines are prominent during the eclipse of the continuum (ϕ = 0.0). The asterisks denote hot spots on the camera face. See Table 1 for details about exposure times, etc.

by ~ 0.07.) The result is illustrated in the top panel of Figure 4. The bottom panel of Figure 4 contains, in addition to the UV data, the nearly simultaneous *UBVRI* data described in the previous section, and the infrared *JHK* values of Longmore *et al.* (1981). The latter were taken when RW Tri was just fainter than $V = 13$ mag, i.e., about the same visual brightness as it was during the *IUE* observations reported here.

Figure 4 clearly shows a broad dip at 2200 Å corresponding to the well-known interstellar feature. We have fitted simple continuum models to the RW Tri data, including the effects of extinction according to the data of Nandy *et al.* (1975). The best fit power law to the distribution of the UV flux, F_λ, has a slope $\alpha = 1.5$ and $E(B-V) = 0.19$ (*top panel*, Fig. 4). No single power law, single blackbody, or linear combinations of these can fit the combined UV, optical, and IR data. Using a simple blackbody disk model (cf. Bath, Pringle, and Whelan 1980), however, we were able to fit the combined data much better; in the bottom panel of Figure 4 we show the best blackbody disk fit, which includes a fixed contribution from the M0 *V* companion star at 2.2 μm (cf. Frank and King 1981). This fit yields an effective disk temperature, $T_* = 9 \times 10^4$ K, a ratio of the outer to inner disk radii, $R_{out}/R_{in} = 50$, and $E(B-V) = 0.25$. The largest deviations from the model are in the *U* band, where the model underestimates the flux, and in the region of the wavy spectral pattern in the far-UV, described in § III*a*.

The total flux between 1200 Å and 22000 Å, not corrected for reddening, is 2×10^{-10} ergs cm^{-2} s^{-1}. Adopting the reddening correction implied by the model fit, the dereddened flux is a factor of ~ 4 higher than this value. The total intrinsic UV, optical and near-IR luminosity of RW Tri is 1.5 $L_\odot$, using the distance of 250 pc derived from the *V* and *K* magnitudes of the secondary star (Bailey 1981).

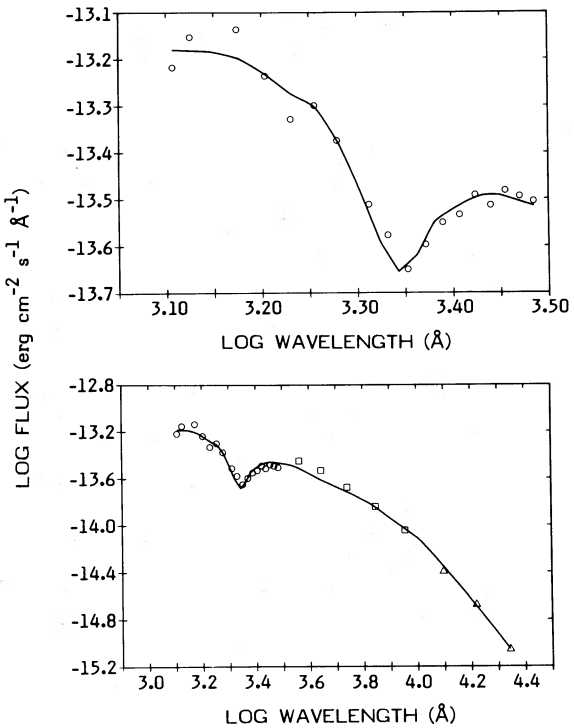

FIG. 4.—The continuum spectrum of RW Trianguli. (*top*) Open circles represent *IUE* data summed over intervals 50 Å to 100 Å wide. The solid line is the best fit power law (including reddening), as described in the text. (*bottom*) Open circles are the *IUE* data; open squares are nearly simultaneous optical *U*, *B*, *V*, *R*, *I* values; and open triangles are the nonsimultaneous near-infrared colors of Longmore *et al.* (1981). The solid line represents the best fit, steady state, blackbody disk model, including reddening. See text for details.

ii) *DQ Herculis*

Our measurements of the weak continuum of DQ Her are of poor statistical quality, and it is not possible to model the continuum with any confidence. When we integrate our data in coarse wavelength bins and correct them for the adopted extinction values, $E(B-V) = 0.1$ of Ferland *et al.* (1984), the normalization and slope of the continuum are in rough agreement with the flat ($F_\lambda \propto \lambda^0$) spectrum of DQ Her derived by the latter authors from a much longer observation of the star. Since Ferland *et al.* do not present a detailed plot of their continuum data, it is impossible to judge how well their data are actually fitted by this model.

iii) *The Mass Accretion Rate*

A mass accretion rate, $\dot{m}$, can be derived for RW Tri based on the steady state, blackbody disk model parameters obtained in § III*b*(i). The prescription of Bath, Pringle, and Whelan (1980) yields a value for $\dot{m}$ of $9 \times 10^{16}(M_1/M_\odot)^{-1}(R_1/5 \times 10^8$ cm$)^3$ g s^{-1}. This estimate, however, depends sensitively on the adoption of the blackbody disk model. If we compare, instead, our UV colors with those of Wade's (1984) model atmosphere disks, we estimate an accretion rate of 1×10^{16} g s^{-1}. Wade's disk model, however, provides a poor fit to the combined UV-plus-optical data (in the sense that it predicts too much flux at *U*, *B*, and *V*).

A method of measuring the mass accretion rate which is independent of spectral fits to the continuum is the eclipse mapping technique described by Horne (1983). Using zero reddening for RW Tri, Horne was unable to get agreement between the measured disk temperature profile and that expected for a steady state disk. The amount of reddening we find substantially modifies Horne's calculated temperature profile, resolving the discrepancy and allowing a determination of $\dot{m}$ to be made. The value of $\dot{m}$ obtained using Horne's data and $E(B-V)$ between 0.2 and 0.3 is about 10^{18} g s^{-1}. The variation in $\dot{m}$ with $E(B-V)$ in this range is less than the factor of 2 uncertainty inherent in the eclipse mapping method.

IV. CONTINUUM LIGHT CURVES

a) RW Trianguli

It is apparent from the spectra presented in Figures 1 and 2 that the UV continuum is depressed during optical eclipse ($\phi = 0.0$), while the emission lines are little changed.

UV light curves can be constructed using the phase-resolved spectra. Figure 5 shows such light curves for the wavelength intervals 1800–1900 Å, 1600–1750 Å, and 1450–1520 Å, using the 1982 January data only. No LWR spectra were taken during the eclipse. In the top panel of Figure 5 we have degraded the temporal resolution of the optical light curve of RW Tri in Figure 2 of Kaitchuck, Honeycutt, and Schlegel (1983) to match the temporal resolution and phases of our UV data, so that the relative optical and UV eclipse depths may be better compared. The light curve of Kaitchuck *et al.* corresponds roughly to the *B* band. The brightness of RW Tri out of eclipse (~ 13.3 mag) and the depth of the eclipse during their observations (~ 2 mag) is quite similar to our own *B* band measurements near the time of the UV observations (cf. § II*b*), thus justifying the comparison of the continuum light curves.

A comparison of the three SWP bands and the *B* band show

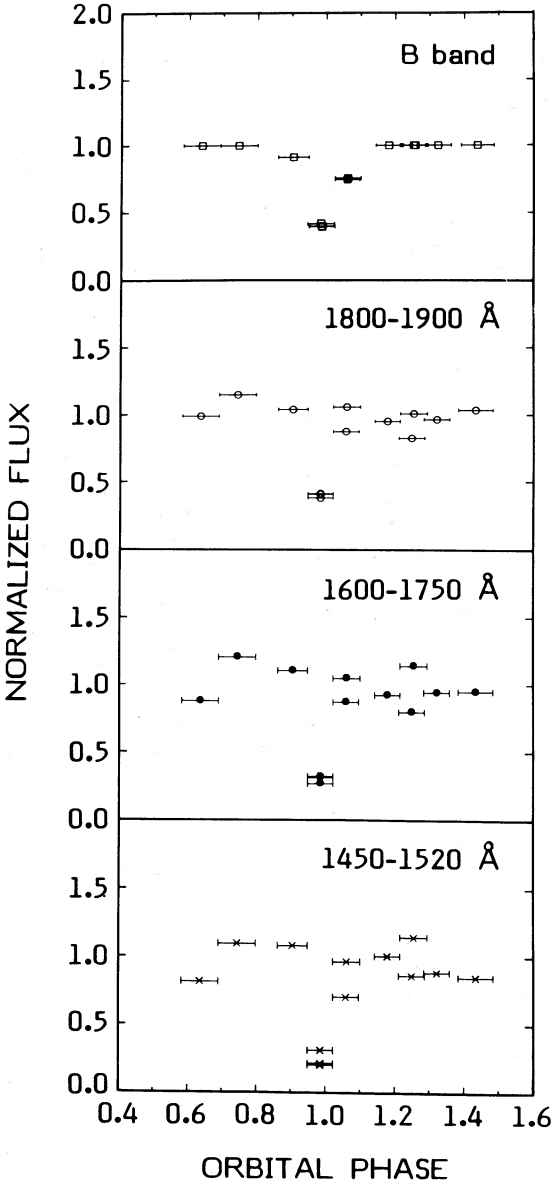

FIG. 5.—The continuum flux as a function of orbital phase in several wavelength intervals. The *B* band data are from Kaitchuck, Honeycutt, and Schlegel (1983), but with coarser binning to mimic the sampling time of the UV data. The light curves show that the eclipse of the continuum becomes progressively deeper at shorter wavelengths.

that the eclipse depth is progressively deeper at shorter wavelengths. This is consistent with the trend apparent in our multiband optical measurements of the eclipse (§ II*b*) and Longmore *et al.*'s (1981) near-infrared eclipse data, and it establishes that the effective size of the eclipsed source becomes smaller towards shorter wavelengths.

b) DQ Herculis

We do not have complete orbital phase coverage for DQ Her. The two good quality SWP spectra taken out of eclipse ($\phi = 0.5$ and $\phi = 0.9$) give values for the average continuum flux level of 1×10^{-14} ergs cm^{-2} s^{-1} Å^{-1}. The eclipse spectrum is integrated over 40 minutes, covering most of the duration of the optical continuum eclipse. The average continuum flux level during eclipse is 0.2×10^{-14} ergs cm^{-2} s^{-1} Å^{-1}, 5 times less than the out-of-eclipse value. In the optical band (using the *B* band data of Schneider and Greenstein 1979), this ratio is 2.6, when the data are sampled with the same time resolution as the UV data. Schneider and Greenstein (1979) noted that the eclipse depth is shallower at longer wavelengths comparing data from 4500 Å to 10200 Å, and the UV observations substantiate this trend. We caution, however, that the comparison of the UV and optical flux ratios in and out of eclipse is only qualitative, since at the low light levels of the DQ Her *IUE* eclipse observation the true continuum flux level may be poorly estimated, owing to the nonlinearity of the camera face and statistical error in subtracting the relatively high detector background.

V. EMISSION-LINE LIGHT CURVES AND LINE PROFILES

a) RW Trianguli

The light curves of the most prominent lines in the RW Tri spectra are shown in Figure 6. They show substantial variabil-

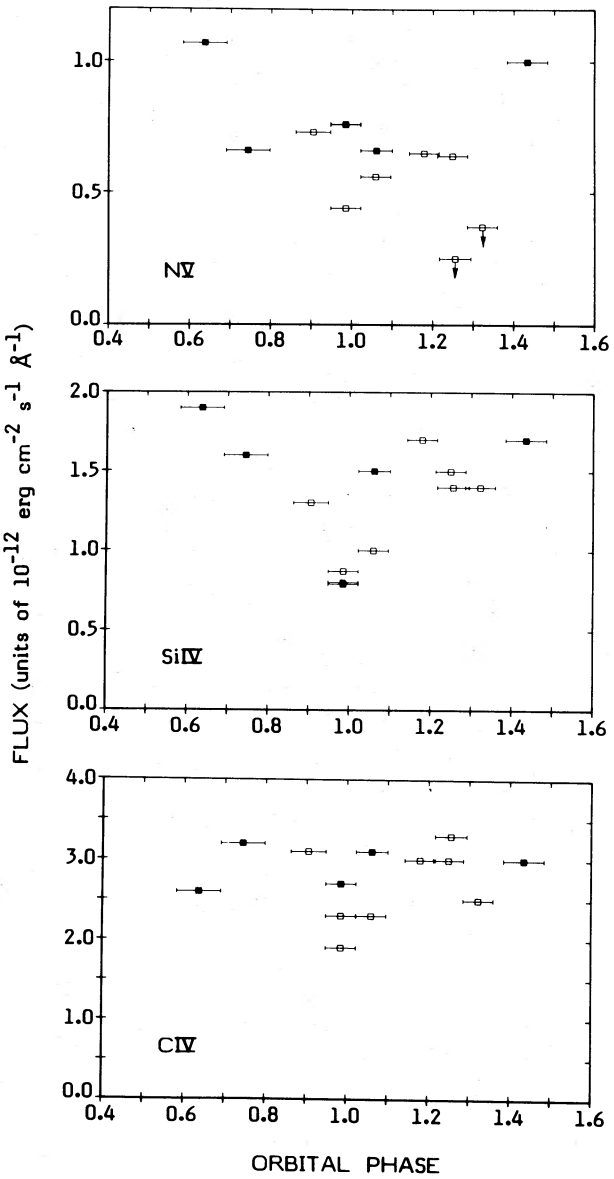

FIG. 6.—Light curves of the most prominent UV spectral lines of RW Trianguli. Data from 1982 January 13/14 are shown with open squares, while data from 1982 January 18 are shown with filled squares.

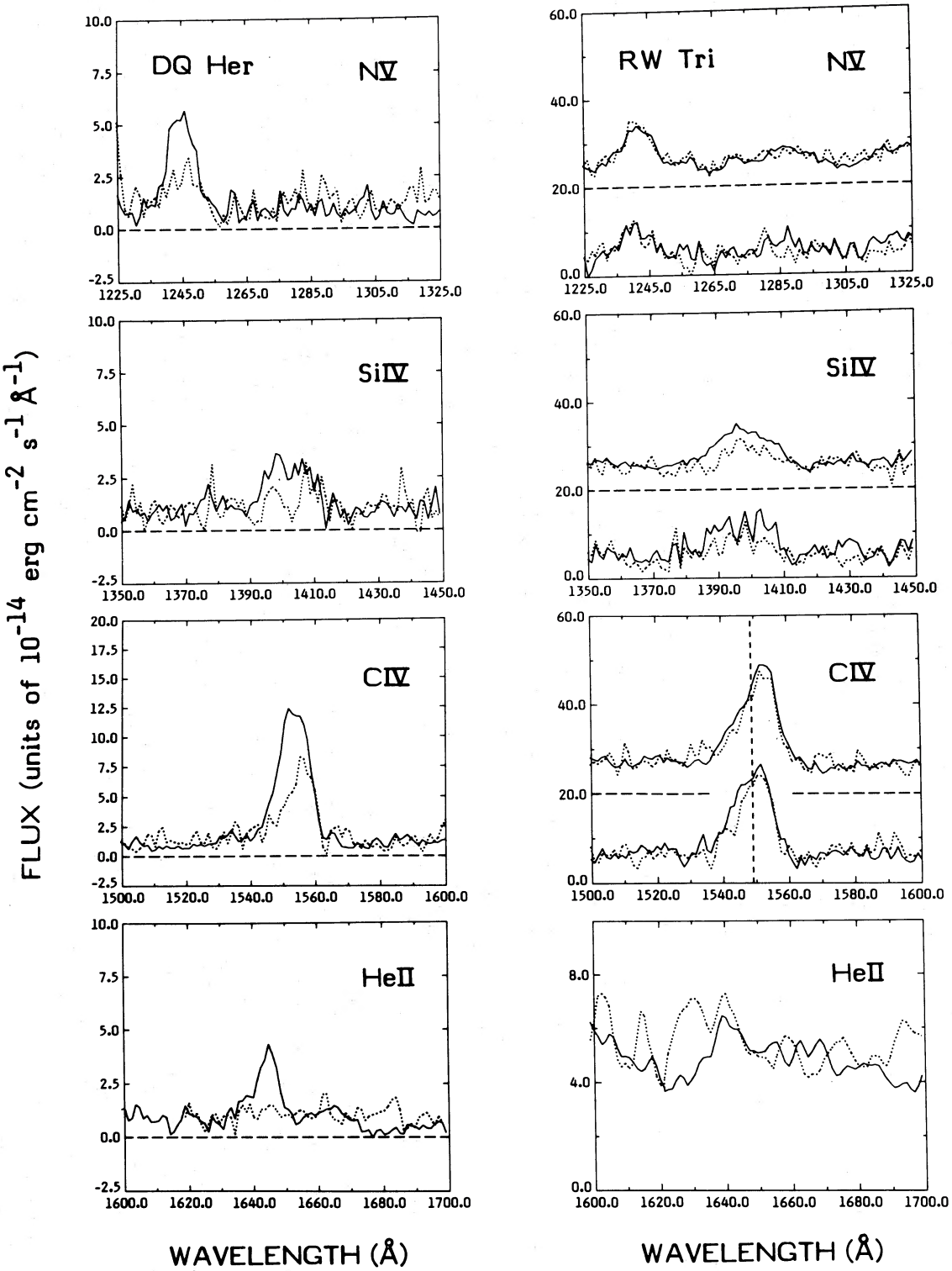

FIG. 7.—Details of the line profiles from summed spectra out of eclipse (*solid lines*) and during eclipse (*dotted lines*). A (different) constant has been added to each of the eclipse spectra to bring the level of the continuum up to the level of the out of eclipse continuum. For RW Tri the observations for different days are separated to demonstrate the repeatability of the profiles: 1982 January 13/14, below; 1982 January 18, offset above with an arbitrary scale factor of 20 units. The horizontal dashed lines denote the zero background level. The short dashed vertical line on the RW Tri C IV figure denotes zero rest wavelength of the doublet, weighted by *gf* factors: the figure illustrates the redshift of the peak.

ity outside of eclipse. To smooth over these fluctuations, we generated time-averaged plots of the line profiles by superposing several measurements outside of eclipse and during the eclipse. The results for N v, Si iv, C iv, and He ii are shown in Figure 7. The two observation epochs of RW Tri in 1982 January have been separated (for all but He ii) to verify that the profiles are repeatable. The C iv profile is very similar in and out of eclipse: (1) it is broad, the red wing extending to ~ 2200 km s^{-1}, and the blue wing extending to -2800 km s^{-1}; (2) it is asymmetric in the sense that the profile is steeper on the redward side; and (3) although the centroid of the emission is at approximately the rest wavelength of the line (weighted by gf factors for the doublet), the peak of the emission is shifted longward. This last point is more clearly illustrated in Figure 8 where we compare the profiles of the C iv line of RW Tri with the same line observed in emission during the optically quiescent phase of the dwarf nova SU UMa. The C iv line of SU UMa does not show asymmetry or substantial velocity shift of the peak, although the line is nearly as broad as in RW Tri. N v, Si iv, and He ii in RW Tri are also shifted to the red with respect to the same lines in SU UMa. Figure 7 demonstrates that RW Tri's lines suffer at most only partial eclipses: the C iv and N v fluxes are at least 80% of their values outside of eclipse, while the Si iv is $\sim 40\%$ of its out-of-eclipse value.

The higher time resolution data of 1982 August suggest that there may be a very localized emission region, smaller in extent than the eclipsed optical continuum region, which undergoes an eclipse. In a phase interval of 0.03 centered exactly on the eclipse the C iv, Si iv, and N v intensities decreased to 60%, 10%, and 40%, respectively, of their values during other phases of the same orbital cycle. This observation is potentially exciting, but, since only a single eclipse measurement was made with this time resolution, it must be treated cautiously, since the observed decrease may just have been caused by flickering in the lines. The results at lower temporal resolution, in contrast, come from averaging several eclipse measurements and are hence more reliable.

b) *DQ Herculis*

Figure 7 illustrates the decrease in the line fluxes during DQ Her's eclipse. He ii may be totally occulted: its eclipse intensity is no more than 30% of the out-of-eclipse value. All the other lines suffer only partial eclipses: C iv remains at 50% of its out-of-eclipse value; Si iv at 30%; and N v at 40%. DQ Her's optical lines enjoy a similar eclipse behavior. Clarke's optical spectroscopy of 1982 August 9 shows that during eclipse He ii $\lambda 4686$ and Hβ are about 27% and 50%, respectively, of their out-of-eclipse values of 2.3×10^{-13} ergs cm^{-2} s^{-1} and 1.4×10^{-13} ergs cm^{-2} s^{-1}.

The FWHM of the C iv line is 9.5 Å, which is smaller than that for either RW Tri (13 Å) or UX UMa (11 Å). The out-of-eclipse lines are symmetric about their centroids, but C iv may be asymmetric during the eclipse: there is a suggestion (cf. Fig. 7) that the low-velocity and blueward components of the line are more eclipsed than the reward components (a similar effect may also be present in RW Tri; cf. the C iv profiles in Fig. 7, but to a lesser extent). The uniform displacement of the centroids by 4 Å to the red may be the result of not centering the star in the slit, as other, much longer exposures of DQ Her do not show this shift (Ferland 1983). The phase coverage of DQ Her is too limited to determine whether flickering in the lines is seriously distorting the line fluxes during the eclipse.

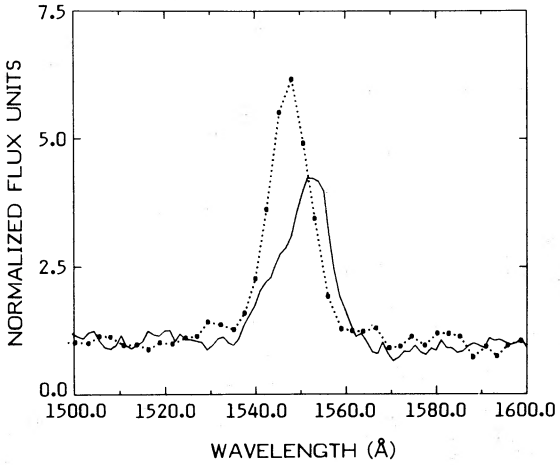

FIG. 8.—Details of the C iv line profiles for RW Trianguli (*solid line*) and SU Ursae Majoris (*dot-dashed line*). The profiles have been normalized by dividing the flux everywhere by the average flux level of the nearby continuum.

VI. DISCUSSION

a) *Background*

The observations presented above concern the eclipsing binaries DQ Her and RW Tri, but this discussion will also make frequent mention of a third, very similar system, UX UMa, which has been similarly studied with *IUE* (Holm, Panek, and Schiffer 1982; King *et al.* 1983). DQ Her, RW Tri, and UX UMa have similar binary periods, colors, short time scale flickering, and eclipse light curves, as noted first by Walker (1963). From the light curves the presence of a gaseous disk, a mass stream from the companion, and a bright spot on the edge of the disk have been inferred. The dominant source of the optical luminosity in all three systems is the accretion disk, which is optically thick in its inner regions (Warner 1976; Mayo, Wickramasinghe, and Whelan 1980; Horne 1983).

An analysis of the optical emission lines of RW Tri and UX UMa has been made by Kaitchuck, Honeycutt, and Schlegel (1983). They conclude that the He ii $\lambda 4686$, which is partially eclipsed during the optical continuum eclipse, is produced in the inner disk or a corona above the inner disk, but that the H i and He i lines, which do not undergo eclipses, are formed in a much more extended volume. All of the optical lines of DQ Her suffer partial eclipses. Changes in the line profile through the eclipse of He ii $\lambda 4686$ suggest that the He ii is produced in the inner disk; the hydrogen Balmer lines are eclipsed earlier than the He ii line and take longer to recover, thus probably originating farther out in the disk (Chanan, Nelson, and Margon 1978; Schneider and Greenstein 1979; Hutchings, Cowley, and Crampton 1979; Young and Schneider 1980).

b) *Summary of Present Results*

Our results on the UV spectral lines of RW Tri and DQ Her from time-resolved observations are as follows:

1. The alkali-like resonance lines, C iv, Si iv, and N v, are observed only in emission.

2. The equivalent widths of the resonance lines in RW Tri are between 20 Å and 40 Å; the equivalent width of He ii is ≤ 3 Å. The equivalent widths of DQ Her's lines are difficult to measure because of the extremely low level of the continuum in this star, but are about 10 times higher than in RW Tri for He ii.

3. In RW Tri the emission peaks are shifted 3–4 Å to the red of the line centroids.

4. The profiles of RW Tri's emission lines are asymmetric in the sense that the redward slope is much steeper than the blueward slope. The edge velocity of the blue wing of the C IV profile in RW Tri extends to -2800 km s^{-1}, but the edge velocity of the red wing is only 2200 km s^{-1}. DQ Her's C IV out-of-eclipse profile is more symmetric, but the eclipse profile looks skewed in the same sense as RW Tri's lines (Fig. 7).

5. When sampled over the same phase interval as the FWHM of the optical continuum eclipse (~ 0.08 in phase), the UV continua of both stars suffer deep eclipses. The lines are eclipsed to a much lesser extent. There is a suggestion in the data that the low-velocity and blueward components of the lines may be eclipsed more than the redward component, but this needs to be confirmed.

6. On one occasion, two successive spectra with 10 minute integration times (or 0.03 of an orbital cycle) were taken of RW Tri during the continuum eclipse. The fluxes of the lines, particularly N V, decreased significantly between the two exposures (cf. the top two panels in Fig. 2). More high time resolution observations are required to determine whether this is due to a narrow eclipse of the lines or to flickering.

7. The fluxes of RW Tri's C IV and N V lines vary by a factor of 2 outside of eclipse. There are no dramatic changes in the line profiles at any phase, including the eclipse. The redward skewness of the profiles is more noticeable in the eclipse spectra and in the spectra of 1982 January 18. The orbital phase coverage is too sparse to determine whether the variability and the asymmetry of the line profiles outside of eclipse is phase dependent.

8. H II λ1640 is prominent in the out-of-eclipse spectrum of DQ Her, but not in RW Tri. During DQ Her's continuum eclipse, the He II flux is reduced by a least a factor of 3, a significantly larger diminution than that shown by any of the other UV spectral lines of this star.

9. Mg II λ2802 is not detected in the summed spectra of either RW Tri or DQ Her, although archival *IUE* data of DQ Her with longer exposure times show that weak Mg II may be present (cf. *IUE* image LWR 7500).

10. There are no detectable intercombination lines in the spectra of either star.

c) *Comparison with UV Lines of Other Cataclysmic Variable (CV) Stars*

The profiles of RW Tri's lines and their eclipse behavior are so similar to that of UX UMa (Holm, Panek, and Schiffer 1981; King *et al.* 1982) that it seems likely that these features Tri and UX UMa and, at least out of eclipse, do not show the obvious asymmetries of the lines of those stars. The eclipses in the lines are deeper in DQ Her, although this comparison is based on only one eclipse measurement of DQ Her, as compared to many eclipse measurements of RW Tri and UX UMa. The continuum of DQ Her is flatter than in the other two stars, and He II is much stronger relative to C IV and N V.

The ratios of the dereddened fluxes for N V: Si IV; C IV: He II are 1: 0.5: 1.2: 0.2 for UX UMa (King *et al.* 1983); 1: 1.7: 2.4: $\leq$0.1 for RW Tri; and 1: 0.7: 3: 0.6 for DQ Her. (Holm, Panek, and Schiffer 1982 give line ratios for UX UMa which are 1: 0.9: 1.9: ?, indicating that these ratios are variable.) The luminosities in the C IV lines of all these stars are roughly comparable, $L_{\rm C\,IV} \approx (4\text{–}10) \times 10^{31}$ ergs s^{-1}, allowing for $E(B-V) =$ 0.25 for RW Tri, 0.1 for DQ Her, and 0.0 for UX UMa, and adopting the distances given by Bailey (1981), Ferland (1980), and Frank *et al.* (1981), respectively.

d) *Physical Conditions in the Line-Emitting Region*

King *et al.* (1983) use the observed ratios of the UV resonance lines in UX UMa to deduce an electron temperature of $T \approx 2 \times 10^4$ K in the emission region. The emitting volume implied by the observed line luminosities if the gas is collisionally ionized is much larger than the entire system. Therefore they conclude that the gas is photoionized. The line ratios in RW Tri yield a similarly low temperature, $T \approx 4 \times 10^4$ K, supporting the case for photoionization in this star as well. Another piece of evidence used by King *et al.* to favor photoionization in UX UMa rests on the observation that N V suffers a deeper eclipse than C IV (collisional ionization would imply similar eclipse behavior). In RW Tri, however, the eclipse behaviors of C IV and N V are similar, although there is flickering in both lines. Such flickering would be expected in a photoionization model if there were fluctuations in the intensity of the ionizing source.

The UV continuum eclipse is deeper than the optical continuum eclipse; this is a natural consequence of the fact that the disk is hotter in its smaller, central regions. The fact that the UV lines are not eclipsed as much as the UV continuum means that the line-emitting region is larger than the inner disk. King *et al.* (1983) compute the scale size of the line emission region in UX UMa to be $\sim(0.5\text{–}1) \times 10^{11}$ cm $\times\, n_{12}{}^{-2/3}$, where n_{12} is the electron density in units of 10^{12} cm^{-3}. RW Tri is so similar to UX UMa in terms of its inclination, binary separation, and size of the secondary star (cf. Frank and King 1981), the very low ratio of C III λ1909 to C III λ1175 ($\leq$0.1), and the shape of its infrared light curve (cf. Longmore *et al.* 1981), that the same

$r_{\rm He\,II} = 1.6$; correcting for $E(B-V) = 0.1$, however, the ratio becomes 2.3. For case B recombination this ratio should be about 6.6 (Seaton 1978). It is possible that λ1640 is substantially more opaque than λ4686, thus reducing $r_{\rm He\,II}$. The emission lines of N, Si, and C are more likely to be produced by collisional excitation than recombination (cf. Jameson, King, and Sherrington 1980).

e) Interpretation of Line Profiles

The asymmetry of the lines and their redshifts are the most obvious features in the spectrum of RW Tri. Similar profiles in the He I λ10830 line in planetary nebulae were interpreted by Vaughan (1968) as originating in a differentially expanding, optically thick wind. In the frame of reference of the emitting gas, a redshifted photon will encounter fewer absorbers than will a violetshifted photon, because of the differential expansion. Thus the opacity of the blueward side of the line is greater than that of the redward side. In some quasars and Seyfert galaxies, too, similar line profiles are observed; one interpretation is that the asymmetry is due to self-absorption of the line photons in circumnuclear clouds expanding radially from a central, photoionizing source (Capriotti, Foltz, and Byard 1981). In both examples no velocity-shifted absorption is observed because the line-emitting material is not seen in projection against a continuum source. For CVs viewed along the plane of the accretion disk these conditions are satisfied if the line emission originates in an optically thick wind accelerated outward from the inner disk/white dwarf region, so that much of the observed emission comes from well above the plane of the disk. The extremely high edge velocities of the lines and the high ionization states of the observed species are also compatible with the lines being formed in a wind which is ionized by a high-energy source close to the compact star. It is important to confirm whether or not the low-velocity material is the most strongly occulted during eclipses (viz., see § V*b*, point 7) because such behavior would be consistent with an accelerating flow originating from this vicinity.

Both the He II λ4686 and λ1640 could be produced in a wind (cf. Klein and Castor 1978 for a discussion of He II line formation in expanding atmospheres). The widths of both the optical and UV He II lines are narrow compared to the other emission lines (see, e.g., Kaitchuck, Honeycutt, and Schlegel 1983 concerning the relatively narrow λ4686 in RW Tri which does not mimic Keplerian motion in the inner disk). If these lines are produced by recombination the line emissivity per unit volume is proportional to the density squared. Since most of the emission comes from the lower part of the wind where the velocity is small, the wings on these lines will not extend to as high velocities as the wings on the lines formed farther out in the wind.

The present observations do not uniquely determine the geometry of the wind. If the wind is expelled in a jet rather than spherically, the component of the velocity projected toward our line of sight will be smaller for higher inclination angles. In fact, the two high-inclination systems reported here do have lower blue edge velocities than those reported for more pole-on systems like RW Sex (Greenstein and Oke 1982) and TW Vir (Paper I). This result is inconclusive because the extreme velocity of the absorption edge is difficult to measure in low-resolution *IUE* spectra of faint systems. In addition, data are very limited on the inclinations of all but the most highly inclined systems.

f) The Mass Loss Rate

To date, all derivations of mass loss rates in the winds of cataclysmic variables have relied on fitting the velocity-shifted absorption part of the UV resonance line profiles to the theoretical profiles of Castor and Lamers (1979) and Olson (1982) for hot stars (e.g., Paper I; Greenstein and Oke 1982; Krautter *et al.* 1981; Klare *et al.* 1983). The model assumes spherical symmetry and single resonance scattering in the lines. The absorption part of the theoretical profiles is much less sensitive to the adopted velocity law than the emission part of the profile and, at least away from the line center, provides an estimate of the optical depth of the wind, and hence an estimate of the mass loss rate (when the ionization fractions and length scale of the acceleration are known). It was pointed out in Greenstein and Oke (1982) and in Paper I that the emission and absorption components of CV line profiles cannot be fitted simultaneously with the theoretical profiles. A similar situation exists for RW Tri whose resonance line profiles bear no resemblance to any of the theoretical profiles. This implies that the assumption of a spherically symmetric wind and/or the assumption of resonance scattering is not appropriate for the emission-line region in these stars. This means that, at least in the context of current stellar wind models, the mass loss rates in cataclysmic variable stars cannot be determined from either the emission components alone or the ratio of the emission to the absorption component.

g) The Photoionizing Spectrum

The various X-ray nebular models published by Kallman and McCray (1982) are potentially interesting in the present context since X-ray emission is a common feature of cataclysmic variables (Córdova and Mason 1983). In these models the ion abundances and temperature depend only on the shape of the local ionizing spectrum and on the ionization parameter $\xi = L_x/(nr_0^2)$. Here L_x is the X-ray luminosity, n is the density of the ionized medium, and r_0 is the mean square distance from the continuum source to the line-forming gas.

The optical depth of the individual ions, τ, can be estimated by fitting the absorption part of the line profiles of CVs with the theoretical models of Castor and Lamers (1979). The range of optical depths measured for most cataclysmic variables is $\tau \approx 0.2$–5. From τ and the measured edge velocities, a lower limit to the column density, $N(C^{+3})$, of order 10^{16} cm^{-2} can be inferred (utilizing eq. [1] in Castor and Lamers 1979). Assuming a solar abundance of carbon in the wind and an ion fraction of unity, the column density of hydrogen is at least 3×10^{19} cm^{-2}. Using Model 2 of Kallman and McCray (1982) and the range of measured τ, we can determine the values of L_x which will produce C IV and Si IV in the ratios observed. If a 10 keV ionizing spectrum is adopted, the range of permissible L_x is 10^{30}–10^{32}, which is in the range of the observed hard X-ray luminosities (Córdova and Mason 1983). These models, however, cannot simultaneously produce all of the observed ion ratios (i.e., N V to C IV, as well as C IV to Si IV).

Kallman (1983) has generated more detailed X-ray nebular models to attempt to fit all the observed relative ion fractions of the wind-emitting dwarf nova, TW Vir. A 10 keV bremsstrahlung model with an ionization parameter $\xi \approx 10$ works if absorption of $N_{\rm H} = 3 \times 10^{18}$ cm^{-2} is included. Using this ionization parameter and the continuity equation, Kallman derives a mass loss rate for TW Vir of $\sim 10^{-10}\ M_\odot$ yr^{-1}, which is independent of the OB star wind analogy used in Paper I. The energy in the wind is, then, $\sim 10^{33}$ ergs s^{-1}.

Once ξ has been derived, the ion fractions, g_i, are determined from the X-ray nebular model; if $\xi \sim 10$, then $g_i \ll 0.1$ for the observed species C IV, N V, and Si IV. Then r_0 can be derived from $\xi = L_x\, g_i/(N_C r_0)$. Using canonical values for all of these numbers (i.e., $\tau \approx 0.5$, $L_X \approx 10^{31}$ ergs s^{-1}), r_0 is of order 10^9 cm, and the density in the region where the wind is ionized is $n = N_c/(g_i r_0) \approx$ a few $\times\ 10^{11}$ cm^{-3}.

There are several problems with the hard X-ray photoionization model. First, the derived length scale for the acceleration, r_0, is smaller by two orders of magnitude than the emission-line region scale size determination of King *et al.* (1983; cf. § VI*d*). The X-ray nebular model includes only recombination emission from Si V and C V, and only the absorption component of the line profiles are modeled successfully. Clearly there must be additional contributions to the line emission; collisional excitation of C IV and Si IV is one possibility.

Second, the observed hard X-ray luminosity of RW Tri is at least 10 times lower than the (dereddened) luminosities of the detected UV lines and may be a hundred times lower than the energy flux in the entire wind (i.e., $L_x \leq 10^{31}$ ergs s^{-1}, from a marginal *Einstein* detection communicated by Patterson 1983). This suggests that unless the hard X-ray source is mostly occulted by the disk, there is not enough energy in this component to accelerate the wind. A similar situation occurs for UX UMa, whose X-ray flux is also quite low (Becker 1981). This discrepancy is serious and most likely implies that it is the ultraviolet or extreme ultraviolet photons emitted in the inner disk that provide the necessary energy to accelerate the wind.

The hard X-ray photoionization model is almost certainly not unique: an inspection of Figure 2 in Kallman (1983) shows that a much lower temperature blackbody with $T \approx 10^5$ K also gives relative ion fractions which are marginally consistent with those observed. In addition, all of the models investigated by Kallman assume cosmic abundances and a homogeneous wind, neither of which may hold in CV winds. Model atmosphere spectra should be investigated as possible ionization sources. Further observations could make a substantial contribution in determining the photoionizing spectrum: simultaneous, rapid photometric measurements of the wind line profiles and the high-energy continuum (e.g., far-UV, EUV, soft and hard X-ray components) could be searched for the correlated behavior that would affirm the nature of the underlying photoionizing source spectrum.

h) Is There a Wind in DQ Heculis?

The partial occultation of the UV resonance lines of DQ Her suggest that part of the line-emitting region extends above and below the disk. However, the out-of-eclipse line profiles of DQ Her are not as dramatically asymmetric as those of UX UMa or RW Tri. This might indicate that a corona rather than an accelerating wind is the dominant contributor to the UV line radiation. The absence of a wind may be because the mass accretion rate is too low for radiative acceleration of a wind or because the inner disk is disrupted by the white dwarf's magnetic field (Katz 1975). An alternate possibility is suggested by a comparison of the eclipse profile of C IV with the out-of-eclipse profile (Fig. 7). While the latter is fairly symmetric, the former appears to be skewed to the red in the same sense as the profiles of RW Tri and UX UMa. This suggests that a wind may be present but contributes only part of the total line emission. Data obtained with higher spectral and temporal resolution should resolve this question.

VII. CONCLUSIONS

We have attempted to further delineate the location, geometry, and physical conditions of the winds in cataclysmic variable stars by studying two systems in which prominent eclipses of the optical continuum reveal that the accretion disk is viewed almost edge on. Thus the companion star can be used to probe the geometry of the wind. We found that one of these stars, RW Tri, has an asymmetric emission-line spectrum very similar to that of UX UMa, which is the only other eclipsing cataclysmic variable that has been investigated in a similar way in the ultraviolet. The shapes of the lines, their high edge velocities, and their eclipse behavior indicate that they are produced in a wind which is accelerated from the central regions of the disk. There is more energy in the detected UV lines than in the observed hard X-ray component. Therefore, while X-rays may ionize the wind, the radiative force to accelerate the wind must be provided by lower energy photons. If the wind is photoionized we could expect to detect (with the next generation of more sensitive UV instruments) correlated changes in the intensity of the line profiles and the spectral component responsible for the ionization. The other edge-on cataclysmic variable reported here, DQ Her, also has an extended UV line-emitting region, but it is not clear whether the emitting gas is being expelled from the system.

We are very grateful to Drs. John Clarke, John Middleditch, and William Priedhorsky for making nearly simultaneous optical measurements of these objects. We acknowledge helpful conversations with Drs. Keith Horne and Andrew King concerning various aspects of the interpretation, and William Priedhorsky for numerous critical comments on the original text. F. A. C. acknowledges the U.S. Department of Energy and K. O. M. acknowledges the U.K. Science and Engineering Research Council for support of this research. F. A. C. thanks Professor J. L. Culhane and the Mullard Space Science Laboratory for its hospitality during her tenure at MSSL as a NATO post-doctoral fellow, when much of this paper was written.

REFERENCES

Africano, J. L., Nather, R. E., Patterson, J., and Robinson, E. L. 1978, *Pub. A.S.P.*, **90**, 568.
Bailey, J. 1981, *M.N.R.A.S.*, **197**, 31.
Bath, G. T., Pringle, J. E., and Whelan, J. A. J. 1980, *M.N.R.A.S.*, **194**, 967.
Becker, R. 1981, *Ap. J.*, **251**, 626.
Capriotti, E., Foltz, C., and Byard, P. 1981, *Ap. J.*, **245**, 396.
Castor, J. I., and Lamers, H. J. G. L. M. 1979, *Ap. J. Suppl.*, **39**, 481.
Chanan, G. A., Nelson, J. E., and Margon, B. 1978, *Ap. J.*, **226**, 963.
Córdova, F. A., and Mason, K. O. 1982, *Ap. J.*, **260**, 716 (Paper I).
———. 1983, in *Accretion Driven Stellar X-ray Sources*, ed. W. H. G. Lewin and E. P. J. Van den Heuvel (Cambridge: Cambridge University Press), p. 147.
Ferland, G. J. 1980, *Observatory*, **100**, 166.
Ferland, G. J. 1983, private communication.
Ferland, G. J., Williams, R. E., Lambert, D. L., Shields, G. A., Slovak, M., Gondhalekar, P. M., and Truran, J. W. 1984, *Ap. J.*, **281**, 194.
Finley, D. S., Basri, G., and Bowyer, S. 1984, in *Future of Ultraviolet Astronomy Based on Six Years of IUE Research*, in press.
Frank, J., and King, A. R. 1981, *M.N.R.A.S.*, **195**, 227.
Frank, J., Kingk, A. R., Sherrington, M. R., Jameson, R. F., and Axon, D. 1981, *M.N.R.A.S.*, **195**, 505.
Greenstein, J. L., and Oke, J. B. 1982, *Ap. J.*, **258**, 209.
Guinan, E. F., and Sion, E. M. 1982, *Ap. J.*, **258**, 217.
Holm, A., and Crabb, W. 1979, *NASA IUE Newsletter*, No. 7, p. 40.
Holm, A. V., Panek, R. J., and Schiffer F. H., III. 1982, *Ap. J. (Letters)*, **252**, L35.

Horne, K. 1983, Ph.D. thesis, California Institute of Technology.
Hutchings, J. B. 1980, *Pub. A.S.P.*, **92**, 458.
Hutchings, J. B., Cowley, A. P., and Crampton, D. 1979, *Ap. J.*, **232**, 500.
Jameson, R. F., King, A. R., and Sherrington, M. R. 1980, *M.N.R.A.S.*, **191**, 559.
Kaitchuck, R. H., Honeycutt, R. K., and Schlegel, E. M. 1983, *Ap. J.*, **267**, 239.
Kallman, T. R. 1983, *Ap. J.*, **272**, 238.
Kallman, T. R., and McCray, R. 1982, *Ap. J. Suppl.*, **50**, 263.
Katz, J. I. 1975, *Ap. J.*, **200**, 298.
King, A. R., Frank, J., Jameson, R. F., and Sherrington, M. R. 1983, *M.N.R.A.S.*, **203**, 677.
Klare, G., Krautter, J., Wolf, B., Stahl, O., Vogt, N., Wargau, W., and Rahe, J. 1982, *Astr. Ap.*, **113**, 76.
Klein, R. I., and Castor, J. I. 1978, *Ap. J.*, **220**, 902.
Krautter, J., Klare, G., Wolf, B., Duerbeck, H. W., Rahe, J., Vogt, N., and Wargau, W. 1981, *Astr. Ap.*, **102**, 337.
Longmore, A. J., Lee, T. J., Allen, D. A., and Adams, D. J. 1981, *M.N.R.A.S.*, **195**, 825.
Mandel, O. E. 1965, *Peremennye Zvezdy*, **15**, 474.
Mayo, S. K., Wickramasinghe, D. T., and Whelan, J. A. J. 1980, *M.N.R.A.S.*, **193**, 793.
Moffett, T. J., and Barnes, T. G. 1979, *Pub. A.S.P.*, **91**, 180.
Nandy, K., Thompson, G. I., Jamar, C., Monfils, A., and Wilson, R. 1975, *Astr. Ap.*, **44**, 195.
Olson, G. L. 1982, *Ap. J.*, **255**, 267.
Patterson, J. 1983, private communication.
Petterson, J. 1980, *Ap. J.*, **241**, 247.
Pringle, J. E. 1975, *M.N.R.A.S.*, **170**, 633.
Seaton, M. J. 1978, *M.N.R.A.S.*, **185**, 5P.
Schneider, D. P., and Greenstein, J. L. 1979, *Ap. J.*, **233**, 935.
Szkody, P. 1981, *Ap. J.*, **247**, 577.
———. 1982, *Ap. J.*, **261**, 200.
Vaughan, A., Jr. 1968, *Ap. J.*, **154**, 87.
Wade, R. A. 1984, *M.N.R.A.S.*, **208**, 381.
Walker, M. 1963, *Ap. J.*, **137**, 485.
Warner, B. 1976, *Observatory*, **96**, 49.
Wesemael, F., Auer, L. H., Van Horn, H. M., and Savedoff, M. P. 1980, *Ap. J. Suppl.*, **43**, 159.
Young, P. J., and Schneider, D. P. 1980, *Ap. J.*, **238**, 955.

F. A. CÓRDOVA: Los Alamos National Laboratory, M.S. D436, Los Alamos, NM 87545

K. O. MASON: Mullard Space Science Laboratory, Holmbury St. Mary, Dorking, Surrey RH5 6NT, England